Materials Research Proceedings 63 (2026) 160-167 https://doi.org/10.21741/9781644904053-18

Development and Characterization of Supplementary Cementitious Material from Phosphate and Sewage Sludge

Euricia MKHONTO[1,a*], Thandiwe SITHOLE[1,b] and Tebogo MASHIFANA[2,c]

[1]Department of Chemical Engineering, University of Johannesburg, P.O. Box 17011, Doornfontein 2088, South Africa

[2]Department of Chemical Engineering, College of Science, Engineering, and Technology, University of South Africa, C/o Christiaan de Wet & Pioneer Avenue, Florida Campus, Johannesburg 1710, South Africa

[a]euriciam@uj.ac.za, [b]nastassias@uj.ac.za, [c]mashitp@unisa.ac.za

Keywords: Supplementary Cementitious Material, Sewage Sludge, Sustainable Material, Waste Beneficiation

Abstract. The environmental impact associated with cement production highlights the need for alternative low-carbon binders that promote sustainability and circularity. There is limited research that investigates the combined use of sewage sludge (SS) and Phosphate sludge (P) as cement-free supplementary cementitious materials (SCM) that are normally discarded, while they contain pozzolanic elements. This study investigates the feasibility of developing composites with varied proportions of SS and P (40SS:60P, 50SS:50P, 60SS:40P) by evaluating their unconfined compressive strength (UCS) and environmental safety. The raw materials and the developed composite were characterized by their chemical composition using X-ray fluorescence (XRF), mineralogy via X-ray diffraction (XRD), microstructural analysis with a scanning electron microscope (SEM), and functional groups through Fourier-transform infrared spectroscopy (FTIR). The 60SS:40P ratio yielded the highest UCS of 0.89 MPa, with low to no metal leachability below the United States Environmental Protection Agency (USEPA). The analysis showed that the strength was influenced by the formation of C-A-F-S-H, C-S-H, and iron phosphate. The developed composite is suitable for application as backfilling and non-load-bearing blocks. The valorization of SS and P contributes to circularity and minimizes emissions from cement production while advancing SDG 12 (responsible consumption) and SDG 13 (climate action).

Introduction

Cement production accounts for approximately 8% of the world's carbon dioxide (CO_2) emissions from clinkers, a major contributor to climate change (Mirandi and Shirzad, 2025). Supplementary cementitious materials (SCM) have emerged as viable alternatives to lower CO_2 emissions while improving binder properties, such as durability, permeability, and mechanical properties (Nassiri et al., 2025). Rapid urbanization and industrialization generate a notable amount of Sewage sludge (SS) from wastewater treatment and phosphate sludge (P) metal pretreatment processes. These wastes are normally discarded into the landfills, posing a risk to groundwater pollution through heavy metal leaching, which then affects the people consuming it, leading to diseases. However, they contain a significant proportion of silica, alumina, calcium, phosphorus, and iron, which are essential constituent cementitious and pozzolanic reactions, with potential for SCM applications (Jhatial et al., 2023; Zhang et al., 2025).

Studies have shown that when the SS ash is mixed with cement or thermally treated, it exhibits pozzolanic reactivity evident through the formation of hydration products which are suitable for application in mortar, concrete, stabilized materials, and road construction (Chang et al., 2022;

Content from this work may be used under the terms of the Creative Commons Attribution 3.0 license. Any further distribution of this work must maintain attribution to the author(s) and the title of the work, journal citation and DOI. Published under license by Materials Research Forum LLC.

Guo et al., 2022; Xia et al., 2023; Mojapelo et al., 2025). The incorporation of P waste often retards the hydration process, but it successfully produced controlled low-strength materials and ceramic bricks exhibiting good durability (Navarro-Blasco et al., 2015; Muliawan & Astutiningsih, 2018; Karoui et al., 2024; Fadili et al., 2025). Most studies focused on the individual use of SS and P with a heavy reliance on cement. However, there remains a research gap in understanding the behavior of mixing SS and P without cement as SCM. Particularly the reaction mechanism forming the binding products, the effect of mixing ratios on the UCS, and environmental performance are not sufficiently explored. Addressing these gaps presents a novel approach to multi-waste valorization, which supports the climate mitigation plan and the circular economy concept.

This study addresses this gap by investigating the feasibility of utilizing SS and P residue as blended SCM without cement. The composites were prepared at different SS:P ratios to determine the effect on UCS. The obtained composites were characterized by using X-ray fluorescence (XRF), X-ray diffractometer (XRD), Fourier-transform infrared spectra (FTIR), Scanning Electron Microscope (SEM), and Toxicity Characteristic Leaching Procedure (TCLP). The finding shows that the developed composite with a UCS of 0.89 MPa is suitable for applications such as backfilling and non-load-bearing blocks

Material preparation, mix design and methods of testing

XRF composition of the raw materials

Table 1 Chemical composition of P and SS

	SiO_2	Al_2O_3	CaO	P_2O_5	MgO	Fe_2O_3	ZnO
P	0.65	0.34	0.06	25.54	0.19	65.27	7.50
SS	36.59	18.41	20.33	7.30	1.31	6.02	0.46

The P was supplied by a local company that manufactures bolts, and the SS by a local wastewater treatment plant, both in South Africa. They are both residues filtered after leaching phosphorus. The materials were oven-dried for 24hrs at 105℃ to remove the moisture. The P and SS residues were mixed with water at the proportions of 40SS: 60P, 50SS: 50P, and 60SS: 40P (wt.%). The material was mixed with water at a moisture content of 15%, which formed a paste and was cast into a 50x50x50 mm^3 mold. The hardened specimens were covered with foil and cured in the oven at 80℃ for 5 days for gradual strength development while maintaining phase stability. The residue generated from P and SS leaching contained a high proportion of silica, iron, calcium, phosphorus, and alumina, as presented in Table 1. These are elements required for stabilization and development of a composite for application in building and construction (Swierczek et al., 2018).

Unconfined compressive strength testing

The UCS was determined after 5 days using the Matest C104 2.6.3 3000kN at a rate of 0.5 MPa/sec and 15% stop load was applied without shock until the specimen failed then record the maximum load. The UCS was measured on an average of three specimens for consistency and confidence in the results.

Characterization

The elemental composition of the P and SS residue was analyzed by X-ray fluorescence (XRF Rigaku ZSX Primus II). X-ray diffractometer (XRD Ultima IV 40 kV) was used to determine the mineralogical phases. The functional groups of the residue composites were determined by Fourier-transform infrared spectra (FTIR Thermo Scientific, Nicolet iS50 FT-IR). The morphology of the residue composite was studied using a Scanning Electron Microscope (High-resolution SEM; Joel JSM-7900F). The SEM was equipped with AZtec software for Energy-

dispersive X-ray spectroscopy (EDS), Elemental mapping, and phase finder. They were conducted on the raw materials and on the composites after testing the UCS at 5 days.

Toxicity Characteristic Leaching Procedure (TCLP)

The test was conducted as per the United States Environmental Protection (USEPA, 1992) method. An extract solution was prepared using NaOH and CH_3OOH acid with deionized water at pH 4.93±0.005. Optimum composite and extract solution was mixed at 1:20 and the mixture was shaken for 24 h at 25°C±3. The solids were separated from the liquid by filtering with 0.45µm filter paper, and the leachate was further analyzed using ICP-OES.

Results and discussion

P and SS leaching residue composite.

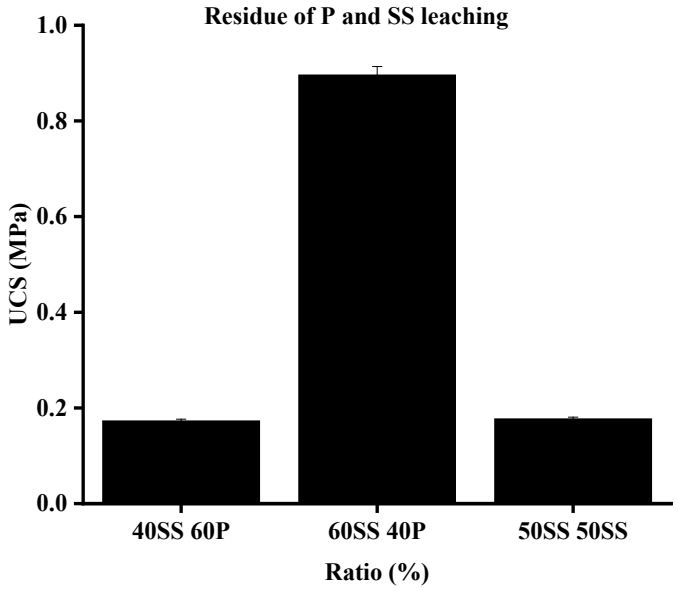


Figure 1 Composite from SS and P-waste residue

Different content of P waste and SS were mixed for stabilization at 40%, 50%, and 60% by weight and the results are presented in Figure 1. The strength of the composites increased with the increasing content/proportion of sewage sludge. The UCS increased by 4.65% when the SS content was increased from 40 to 50% by weight addition. According to ANOVA single-way analysis ($p - value = 0.75 > 0.05$) the addition of SS from 40 to 50% did not have any significant effect on strength development. A significant ($p - value = 0.0028 < 0.05$) change in UCS was observed when SS addition increased by 10% to 60% by weight, with UCS increasing from 0.18MPa to 0.89MPa. The high content of SS improved the strength as it contained a high proportion of calcium, which is responsible for strength development in composite acting as a binder (Ngayakamo et al., 2020). The developed binder is suitable for application as backfilling and non-load-bearing blocks.

Mineralogy of the developed composite P-waste and SS leaching residue

The mineralogy of the P-waste and SS sludge residue mixture from leaching is presented in Figure 2 on the diffraction pattern. The SS showed a crystalline broad diffraction peak between 25° and 30° 2(θ) which was identified as quartz (Q) and a peak of 36° 2(θ) corresponding to apatite containing calcium oxide responsible for strength development. Vivianite was detected at 22° 2(θ). The P-waste exhibits a broad diffraction peak at 20° 2(θ) which was identified as iron phosphate

with all the other peaks dominated by iron and phosphate, the same trend peaks were also observed by Goj et al. (2021) and Maarouf et al. (2021). When the residues are mixed the produced spectrum shows the peak identity of both samples. At 40SS: 60P phases with iron phosphate hydrate and silicon oxide are reported. Calcium iron phosphate broad diffraction peak between 19° and 25° 2(θ) was formed for all the mixed residues. New phases were formed at peak 31° 2(θ) namely parabutlerite, phosphoderite, and magnesium hydrate phosphate for 40, 50, and 60 % SS added in the mixture.

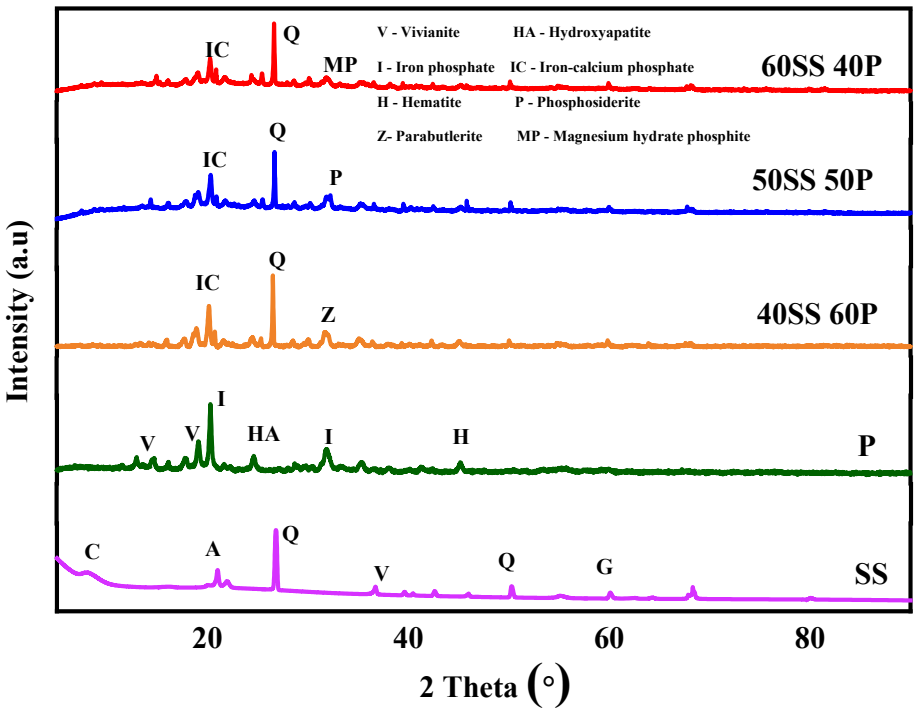


Figure 2 XRD analysis of SS and P-waste residue and composite

Microstructure from SEM of the developed composite P-waste and SS leaching residue

The morphology of the composite developed using leaching residue from P-waste and SS was studied using SEM and the obtained images are presented in Figure 3. The composite which contained 50% SS and 50% P by weight exhibited a structure embedded with spherical and needle-like soft particles. The 60SS: 40P composite by weight showed a compact dense particle embedded with a spherical particle. The 40SS: 60P composite by weight exhibited dispersed particles. The EDS micrographs in Figure 4 showed that the composite is composed of Si, Ca, Fe, Al, and P bonded to O. The Ca: Si and Al: Ca ratios are used as an indication for the formation of hydration products responsible for strength development (Mkhonto et al., 2024). The Ca: Si = 0.5 and Al: Ca = 0.4 are responsible for the reported strength gain. The EDS mapping in Figure 5 confirmed the embedded with a spherical particle on 60SS: 40P composite as Fe which confirms the Fe contained the P-waste residue. The even distribution of the Fe and P shows the reaction between the two elements. The is a high concentration and evenly distribution of Si and Al with traces of Ca, which confirms the reaction of cementitious material C-A-S-H exhibiting the strength reported (Eu et al., 2025).



Figure 3 Microstructure of SS and P-waste residue composite

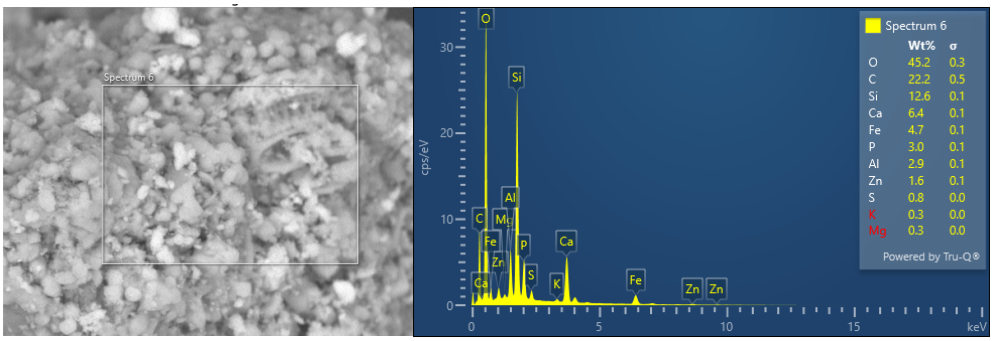


Figure 4 EDS for 60SS 40P composite

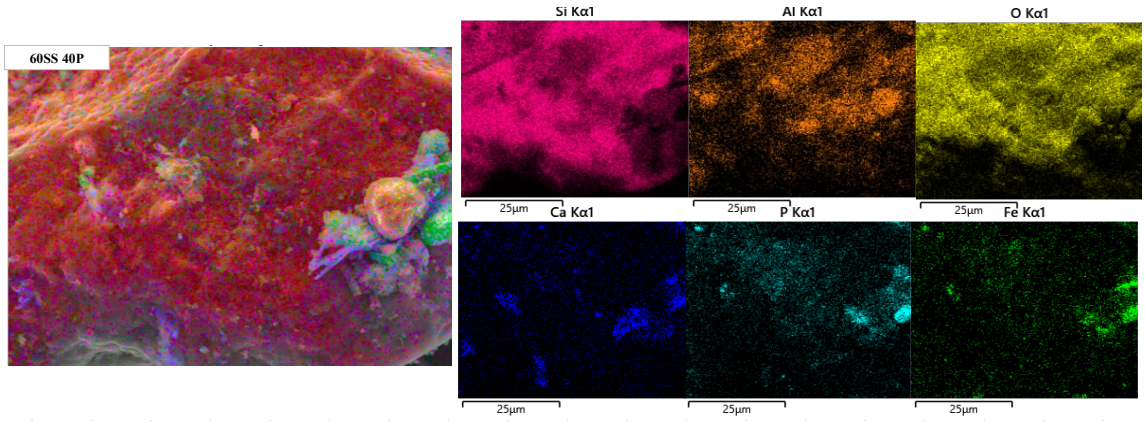


Figure 5 Elemental mapping of 60SS 40P composite

FTIR analysis of the developed composite P and SS leaching residue

The FTIR spectrum of the waste residue composite is presented in Figure 6. The presence of broad absorption bands between 3400-3435 is characterized by the stretching of hydroxyl vibration of water molecules (Maarouf et al., 2021). P-H stretching vibration was absorbed at a wavelength between 2343-2356cm-1, showing the continuous reactivity of phosphorus reaming in both residues (Pu et al., 2021). The vibrational bands reported in 2076 and 2070cm-1 were assigned to the stretching of C-O (Gupta et al., 2016). The absorption band at 1619, 1634, and 1640cm-1 for the different combinations of the residue is assigned to the bending vibration of the H-O-H bonds (Yusuf, 2023). C-H bonds were identified at absorption bands 1399, 1400, and 1384cm-1, these bonds are the ones responsible for the strength development reported for the composite residue (Yang et al., 2018). The vibration band at wavelength 1027-1030cm-1 is ascribed to the stretching of Si-O (Santos et al., 2021). The bands at 779cm-1, and 780cm-1 correspond to Si-O and Al-O bonds (Horgnies et al., 2013). The vibration absorption band at 657cm-1, 675cm-1, 579cm-1,

595cm-1, and 467cm-1 corresponds to S-O stretching (Yusuf, 2023). All the bands representing hydrated phases for a cementitious material were detected with FTIR, this presents the composite of the residue as a cementitious material.

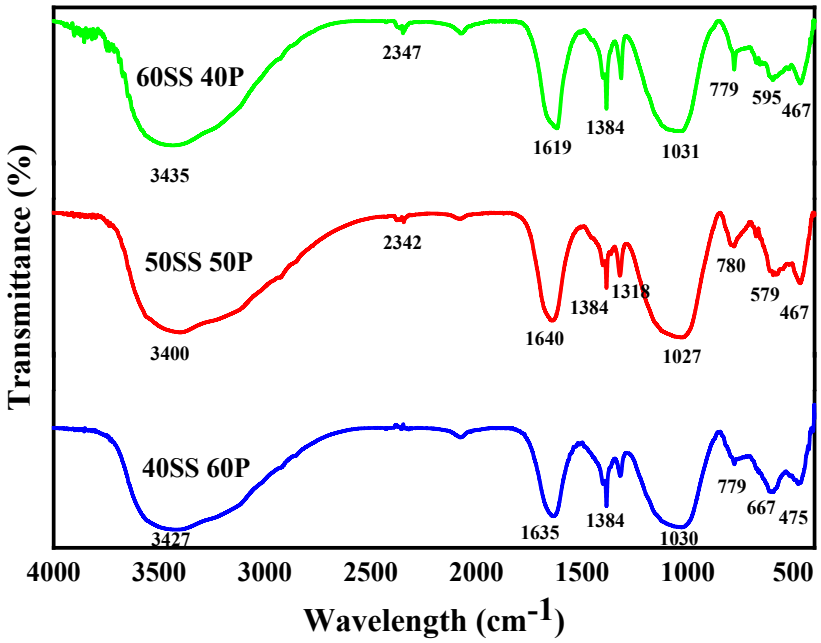


Figure 6 FTIR analysis of SS and P residue composites

TCLP developed composite from P-waste and SS leaching residue

The optimum 60SS 40P composite was evaluated for potential environmental impact using the USEPA toxicity leaching characteristics procedure limits to determine its leachability and prevent environmental pollution. The obtained concentration in comparison with the USEPA allowable concentration is presented in Table 2. The obtained heavy metals concentration for 60SS 40P is below the threshold for USEPA allowable leachable concentrations, with Hg at 0. These results showed that 60SS 40P is safe to be utilized as it will not leach out and contaminate/impact the environment.

Table 2 TCLP metal concentration of 60SS 40P

Metals (mg/L)	As	Ba	Cd	Cr	Pb	Hg	Se
60SS 40P	0.67	0.03	0.01	0.009	0.004	0	0.11
USEPA (1992) limits	5	100	1	5	5	0.2	1

Conclusions

The study showed the feasibility of developing SCM from SS and P. The blended SS and P formed cementitious phases, including C-A-F-S-H, C-S-H, and iron phosphate hydrates without the addition of OPC. The optimum 60SS:40P ratio achieved UCS of 0.89 MPa and exhibited heavy metal leachability below USEPA limit, confirming environmental safety. The developed composite is suitable for application as backfilling and non-load-bearing blocks. The valorization of SS and P contributes to circularity and minimizes emissions from cement production while advancing SDG 12 (responsible consumption) and SDG 13 (climate action).

References

[1] Chang, Z., Long, G., Xie, Y. and Zhou, J.L., 2022. Chemical effect of sewage sludge ash on early-age hydration of cement used as supplementary cementitious material. *Construction and Building Materials*, *322*, p.126116. https://doi.org/10.1016/j.conbuildmat.2021.126116

[2] Dos Santos, V.H.J.M., Pontin, D., Ponzi, G.G.D., e Stepanha, A.S.D.G., Martel, R.B., Schütz, M.K., Einloft, S.M.O. and Dalla Vecchia, F., 2021. Application of Fourier Transform infrared spectroscopy (FTIR) coupled with multivariate regression for calcium carbonate (CaCO3) quantification in cement. *Construction and Building Materials*, *313*, 125413. https://doi.org/10.1016/j.conbuildmat.2021.125413

[3] El Fadili, H., Ait-Khouia, Y., Benzaazoua, M. and Taha, Y., 2025. Symbiotic effects of clayey phosphate sludge and sugar lime on the engineering properties of binary and ternary alkali-activated materials: Harvesting the utilization of industrial by-products. *Construction and Building Materials*, *482*, p.141657. https://doi.org/10.1016/j.conbuildmat.2025.141657

[4] Eu, H., Kim, G., Son, M., Sasui, S., Lee, Y., Choi, H., Kang, S. and Nam, J., 2024. Alkali-Silica Reaction and Residual Mechanical Properties of High-Strength Mortar Containing Waste Glass Fine Aggregate and Supplementary Cementitious Materials. *International Journal of Concrete Structures and Materials*, *18*(1), p.69. https://doi.org/10.1186/s40069-024-00711-x

[5] Goj, P., Wajda, A., Błachowski, A. and Stoch, P., 2021. A new iron-phosphate compound (Fe7P11O38) obtained by pyrophosphate stoichiometric glass devitrification. *Scientific Reports*, *11*(1), 22957. https://doi.org/10.1038/s41598-021-02471-0

[6] Guo, X., Yuan, S., Xu, Y. and Qian, G., 2022. Effects of phosphorus and iron on the composition and property of Portland cement clinker utilized incinerated sewage sludge ash. *Construction and Building Materials*, *341*, p.127754. https://doi.org/10.1016/j.conbuildmat.2022.127754

[7] Gupta, R., Bhardwaj, P., Mishra, D., Mudgal, M., Chouhan, R.K., Prasad, M. and Amritphale, S.S., 2017. Evolution of advanced geopolymeric cementitious material via a novel process. *Advances in Cement Research*, *29*(3), 125-134. https://doi.org/10.1680/jadcr.16.00113

[8] Horgnies, M., Chen, J.J. and Bouillon, C., 2013. Overview of the use of Fourier transform infrared spectroscopy to study cementitious materials. *WIT Trans. Eng. Sci*, *77*, 251-262.

[9] Jhatial, A.A., Nováková, I. and Gjerløw, E., 2023. A review on emerging cementitious materials, reactivity evaluation and treatment methods. *Buildings*, *13*(2), p.526. https://doi.org/10.3390/buildings13020526

[10] Karoui, O., Andrejkovičová, S., Pato, P., Patinha, C., Perná, I., Řimnáčová, D., Hajjaji, W., Ascensão, G., Rocha, F. and Mlayah, A., 2024. Alkali-activated geopolymers based on calcined phosphate sludges and metakaolin. *Environmental Science and Pollution Research*, *31*(32), pp.45138-45161. https://doi.org/10.1007/s11356-024-34025-y

[11] Maarouf, F.Z., Saoiabi, S., Azzaoui, K., Chrika, C., Khalil, H., Elkaouni, S., Lhimr, S., Boubker, O., Hammouti, B. and Jodeh, S., 2021. Statistical optimization of amorphous iron phosphate: inorganic sol–gel synthesis-sodium potential insertion. *BMC chemistry*, *15*, 1-14. https://doi.org/10.1186/s13065-021-00774-x

[12] Marandi, N. and Shirzad, S., 2025. Sustainable cement and concrete technologies: A review of materials and processes for carbon reduction. *Innovative Infrastructure Solutions*, *10*(9), p.408. https://doi.org/10.1007/s41062-025-02213-5

[13] Mkhonto, E., Mashifana, T. and Sithole, N.T., 2024. Synthesis of Acid-Based Fly Ash Geopolymer with Pure Phosphoric Acid Compare with P-Leachate Activator. *Key Engineering Materials*, *980*, pp.109-115. https://doi.org/10.4028/p-ZXKyg9

[14] Mojapelo, K.S., Kupolati, W.K., Burger, E.A., Ndambuki, J.M., Snyman, J., Achi, C.G. and Quadri, A.I., 2025. Durability and Environmental Impact of Wastewater Sludge Ash as a Cement Replacement in Concrete: Challenges and Future Directions. *Materials Circular Economy*, *7*(1), pp.1-19. https://doi.org/10.1007/s42824-025-00172-x

[15] Muliawan, J. and Astutiningsih, S., 2018. Preparation and characterization of phosphate-sludge kaolin mixture for ceramics bricks. *International Journal of Technology*, *9*(2), pp.317-324. https://doi.org/10.14716/ijtech.v9i2.1119

[16] Nassiri, S., Butt, A.A., Zarei, A., Roy, S., Filani, I., Pandit, G.A., Mateos, A., Haider, M.M. and Harvey, J.T., 2025. Opportunities for supplementary cementitious materials from natural sources and industrial byproducts: literature insights and supply assessment. *Buildings*, *15*(17), p.3099. https://doi.org/10.3390/buildings15173099

[17] Navarro-Blasco, I., Duran, A., Perez-Nicolas, M., Fernandez, J.M., Sirera, R. and Alvarez, J.I., 2015. A safer disposal of hazardous phosphate coating sludge by formation of an amorphous calcium phosphate matrix. *Journal of Environmental Management*, *159*, pp.288-300. https://doi.org/10.1016/j.jenvman.2015.05.029

[18] Ngayakamo, B.H., Bello, A. and Onwualu, A.P., 2020. Development of eco-friendly fired clay bricks incorporated with granite and eggshell wastes. *Environmental Challenges*, *1*, 100006. https://doi.org/10.1016/j.envc.2020.100006

[19] Pu, S., Zhu, Z., Song, W., Huo, W. and Zhang, J., 2021. Mechanical and microscopic properties of fly ash phosphoric acid-based geopolymer paste: A comprehensive study. *Construction and Building Materials*, *299*, 123947. https://doi.org/10.1016/j.conbuildmat.2021.123947

[20] Świerczek, L., Cieślik, B.M. and Konieczka, P., 2018. The potential of raw sewage sludge in construction industry–a review. *Journal of cleaner production*, *200*, 342-356. https://doi.org/10.1016/j.jclepro.2018.07.188

[21] Xia, Y., Liu, Y., Wang, L., Song, Z., Sun, C., Zhao, Y., Lu, S. and Yan, J., 2023. Value-added recycling of sludge and sludge ash into low-carbon construction materials: current status and perspectives. *Low-carbon Materials and Green Construction*, *1*(1), p.23. https://doi.org/10.1007/s44242-023-00023-5

[22] Yang, H., Che, Y. and Leng, F., 2018. High volume fly ash mortar containing nano-calcium carbonate as a sustainable cementitious material: microstructure and strength development. *Scientific reports*, *8*(1), 16439. https://doi.org/10.1038/s41598-018-34851-4

[23] Yusuf, M.O., 2023. Bond characterization in cementitious material binders using Fourier-transform infrared spectroscopy. *Applied Sciences, 13(5), 3353. https://doi.org/10.3390/app13053353*

[24] Zhang, Y., Nie, S. and Liu, C., 2025. Phosphorus slags: Structural insights, dissolution behavior, and potential as sustainable supplementary cementitious materials. *Chemical Engineering Journal*, *507*, p.160463. https://doi.org/10.1016/j.cej.2025.160463